Journal of the Korean Physical Society, Vol. 65, No. 1, July 2014, pp. 111∼116

Population Balancing with Species Switching

Juyong Song and Junghyo Jo*
Asia Pacific Center for Theoretical Physics, Pohang 790-784, Korea
and Department of Physics, Pohang University of Science and Technology, Pohang 790-784, Korea

Danh-Tai Hoang and Jongwook Kim
Asia Pacific Center for Theoretical Physics, Pohang 790-784, Korea

(Received 10 April 2014, in final form 27 May 2014)

Biological organisms are composed of cells differentiated from stem cells. Emerging evidence suggests phenotypic switches of differentiated cells, called transdifferentiation, during development and under pathophysiological conditions. To examine the role of transdifferentiation for population balances, we construct a stochastic model mapped into urn problems. When a colored ball is drawn from an urn, one additional ball with the same color is put into the urn in Polya's urn scheme while the drawn ball is replaced by another ball with different color in Ehrenfest's urn scheme. Our population balance model is a mixture of the two classic urn problems corresponding to cell replication and transdifferentiation. Because a dominant population is more likely to be drawn, the preferential replication and transdifferentiation of the dominant population contribute to increasing and decreasing the gap between the two populations, respectively. Therefore, their competition determines population balancing. We analyze the dependence of population dynamics on the replication and the transdifferentiation rates of each population. Finally, experimentally probing the event of transdifferentiation is a challenging problem because it is indistinguishable from death of one cell type and concurrent replication of another cell type. Our analysis suggests that transdifferentiation generates fewer fluctuations in population dynamics than the combined events of cell death and replication do.

PACS numbers: 87.10.Mn, 87.23.Cc, 05.10.Gg
Keywords: Transdifferentiation, Polya's urn, Ehrenfest's urn, Fluctuation, Biological modeling
DOI: 10.3938/jkps.65.111

I. INTRODUCTION

Stem cells differentiate into various cell types during development. Unlike the general notion that differentiated cells permanently maintain their phenotypes, recent evidence has shown that differentiated cells can change their phenotypes [1–3]. The phenotypic switch of cells, called *transdifferentiation*, occurs in normal development, metamorphosis, and regeneration processes [4, 5]. Its therapeutic potential has attracted clinical attention to replacing injured cells with healthy neighboring cell types [6]. Considerable efforts have been devoted to generate pancreatic β cells in diabetes [7, 8], cardiomyocytes in heart diseases [9], and neurons in neurodegenerative diseases [10].

The real conversion of cell types is technically hard to probe because it can be confused with the death of one cell type and the concurrent replication of another cell type. A lineage tracing method using fluorescent materials has been applied to demonstrate the event of transdifferentiation and to show its regulation by master switch genes [11]. Although the genetic and the molecular mechanisms of transdifferentiation have been studied in detail, its contribution to population balancing in tissues has not received much attention. Here, we construct a population dynamics model considering transdifferentiation. In particular, we consider transdifferentiation to be a stochastic process [12]. Population dynamics has been intensively studied in biology [13], and it has also been considered in the phenotypic change of bacteria [14].

In this study, we map the population dynamics of cells into urn problems, which have been widely applied in various fields [15]. When a colored ball is drawn from an urn, one additional ball with the same color is put into the urn in Polya's urn scheme while the drawn ball is replaced by another ball with different color in Ehrenfest's urn scheme. The ball replacements in the two classic urn schemes can represent replication and transdifferentiation of cells, respectively. Based on the stochastic model, we examine the dependence of the population

*E-mail: jojunghyo@apctp.org

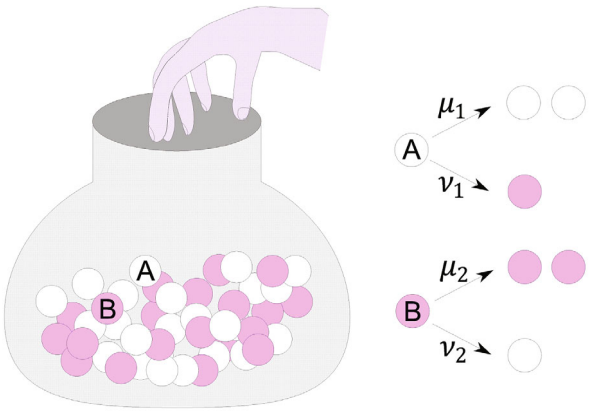

Fig. 1. (Color online) Population dynamics as an urn process. When one draws an A ball, one puts back one additional A ball with μ_1 probability or switches it with a B ball with ν_1 probability. The same applies for drawing a B ball. Ball addition and switching in an urn corresponds to cell replication and transdifferentiation in a tissue.

balance of cells on their replication and transdifferentiation rates. In addition to the model considering transdifferentiation, we develop another model considering cell death instead of transdifferentiation. The switch of cell type can be experimentally confused with the death of one cell type and the concurrent replication of another cell type. Therefore, we examine a distinctive feature of two confusable models: (i) the switch model and (ii) the death model.

II. MODEL

We consider the population dynamics of the cells in tissues as ball replacement events in an urn. Cell replication corresponds to ball addition in Polya's urn scheme while cell transdifferentiation corresponds to ball replacement in Ehrenfest's urn scheme [15]. Suppose we have an urn containing two kinds of balls, A and B balls, representing two cell types. Once we draw an A ball, we may put back one additional A ball with a probability μ_1 or replace it with a B ball with a probability ν_1. The same applies for drawing a B ball. In general, A and B cells (balls) have different replication rates, μ_1 (A→AA) and μ_2 (B→BB), and different switch rates, ν_1 (A→B) and ν_2 (B→A), respectively (Fig. 1). During the drawing process, a dominant population is more likely to be drawn. Therefore, replication makes a dominant population more dominant while switching makes a dominant one less dominant. Their competition determines the population balance of the two cell types. If a is defined as the number of A cells and b as the number of B cells, the temporal change in the population distribution can be described by a master equation:

$$\begin{aligned} &P(a,b;t+1)-P(a,b;t)= \\ &\mu_1\frac{a-1}{a+b-1}P(a-1,b;t)+\mu_2\frac{b-1}{a+b-1}P(a,b-1;t) \\ &+\nu_1\frac{a+1}{a+b}P(a+1,b-1;t)+\nu_2\frac{b+1}{a+b}P(a-1,b+1;t) \\ &-(\mu_1+\nu_1)\frac{a}{a+b}P(a,b;t)-(\mu_2+\nu_2)\frac{b}{a+b}P(a,b;t). \end{aligned} \tag{1}$$

The population distribution (a,b) at time $t+1$ can be realized by replicating one A cell from the $(a-1,b)$ distribution at time t, replicating one B cell from the $(a,b-1)$ distribution, switching one A cell with B cell from the $(a+1,b-1)$ distribution, or switching one B cell with A cell from the $(a-1,b+1)$ distribution. Opposite to these in-fluxes in the master equation, the replication and the switching of A and B cells from the (a,b) distribution contribute to out-fluxes of the population distribution (a,b). The first term in Eq. (1) represents the contribution from the replication of A cells. Its transition rates, $\mu_1(a-1)/(a+b-1)$, can be interpreted as a total probability obtained by multiplying the selection probability of A cells from among $(a-1)$ numbers of A cells and b numbers of B cells, and the replication probability of a selected A cell. Other terms can be similarly interpreted. Note that the master equation is a good approximation for the population dynamics of cells with small replication and switch rates where simultaneous replication and switching of multiple cells are negligible.

Because we are particularly interested in the total population size and the population gap between two cell types, we change our variables to $x=a+b$ and $y=a-b$. In the continuous limit of long time t and large numbers a and b, we can obtain a Fokker-Planck equation by conducting Taylor expansion of Eq. (1):

$$\begin{aligned} \partial_t P &= -\partial_x v_x P-\partial_y v_y P \\ &\quad +\frac{1}{2}\partial_x^2 D_{xx}P+\frac{1}{2}\partial_y^2 D_{yy}P+\partial_x\partial_y D_{xy}P, \end{aligned} \tag{2}$$

where the drift and the diffusion terms are

$$v_x = \bar{\mu}+\Delta\mu\frac{y}{x}, \tag{3}$$

$$v_y = \Delta\mu-2\Delta\nu+(\bar{\mu}-2\bar{\nu})\frac{y}{x}, \tag{4}$$

$$D_{xx} = \bar{\mu}+\Delta\mu\frac{y}{x}, \tag{5}$$

$$D_{yy} = \bar{\mu}+4\bar{\nu}+(\Delta\mu+4\Delta\nu)\frac{y}{x}, \tag{6}$$

$$D_{xy} = \Delta\mu+\bar{\mu}\frac{y}{x}, \tag{7}$$

with redefined parameters $\bar{\mu}=(\mu_1+\mu_2)/2$, $\bar{\nu}=(\nu_1+\nu_2)/2$, $\Delta\mu=(\mu_1-\mu_2)/2$, and $\Delta\nu=(\nu_1-\nu_2)/2$. The Fokker-Planck equation can describe the average behaviors of x and y, and their fluctuations [16].

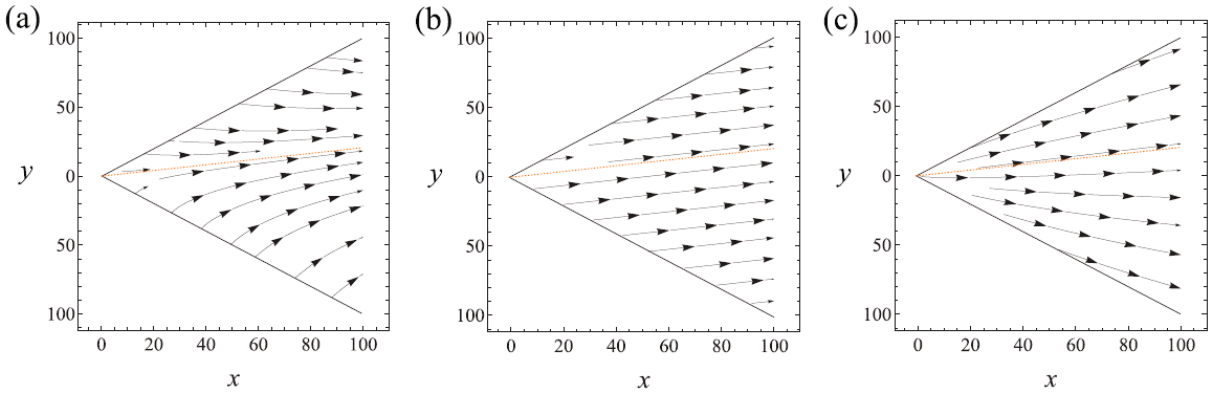

Fig. 2. (Color online) Phase portraits of the population dynamics. Arrows represent vector fields $(\dot{x}, \dot{y})$, given total population size x and population gap y, which are defined as $x = a + b$ and $y = a - b$ for a numbers of A cells and b numbers of B cells. Note $x \geq |y|$. The population dynamics depends on four parameters: the replication rates μ_1 (A→AA) and μ_2 (B→BB) and switch rates ν_1 (A→B) and ν_2 (B→A). Plots are for (a) the switch-dominant condition ($\mu_1 = 0.051, \mu_2 = 0.021$), (b) the critical condition ($\mu_1 = 0.078, \mu_2 = 0.048$), and (c) the replication-dominant condition ($\mu_1 = 0.215, \mu_2 = 0.185$). Here, the switch rates are fixed as $\nu_1 = 0.031$ and $\nu_2 = 0.029$. The dotted orange lines represent a converging ratio $y/x = z^* = (-\bar{\nu} + \sqrt{\bar{\nu}^2 + \Delta\mu(\Delta\mu - 2\Delta\nu)})/\Delta\mu$, with $\Delta\mu = (\mu_1 - \mu_2)/2$, $\bar{\nu} = (\nu_1 + \nu_2)/2$, and $\Delta\nu = (\nu_1 - \nu_2)/2$. Note that the three plotted conditions have equivalent values of $\Delta\mu$, $\bar{\nu}$, and $\Delta\nu$.

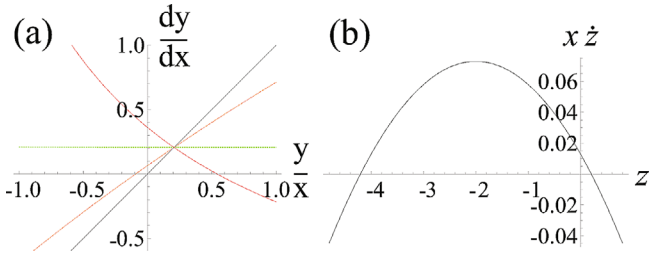

Fig. 3. (Color online) Local slope and fixed point in the population dynamics. The total population size and the population gap are defined as $x = a+b$ and $y = a-b$, respectively, with a numbers of A cells and b numbers of B cells. (a) Local slope dy/dx versus y/x: switch-dominant condition (solid red line), critical condition (dashed green line), and replication-dominant condition (dotted orange line). Note the thin black solid line, $dy/dx = y/x$, is plotted for guidance. (b) The dependence of the velocity $z = y/x$ on z. Here, a positive z^* exists as a stable fixed point for $\dot{z}(z^*) = 0$. A negative z^* also exists as an unstable fixed point, but it is out of range for $|z| \leq 1$. Specific parameter values of the replication and the switch rates for A and B cells are referred to the legend in Fig. 2.

III. AVERAGE BEHAVIOR OF THE POPULATION BALANCE

The drift terms in the Fokker-Planck equation of Eq. (2) describe the average behavior of the population balance. The time derivatives of the average x and y correspond to the drift velocities v_x and v_y:

$$\dot{x} = \bar{\mu} + \Delta\mu \frac{y}{x}, \tag{8}$$

$$\dot{y} = (\Delta\mu - 2\Delta\nu) + (\bar{\mu} - 2\bar{\nu}) \frac{y}{x}. \tag{9}$$

We can obtain exact solutions for a simple case where two cell types have the same replication and switch rates, $\bar{\mu} = \mu_1 = \mu_2$ and $\bar{\nu} = \nu_1 = \nu_2$ with $\Delta\mu = \Delta\nu = 0$:

$$x(t) = x(0) + \bar{\mu}\, t, \tag{10}$$

$$y(t) = y(0)\Big[1 + \frac{\bar{\mu}\, t}{x(0)}\Big]^{1 - 2\bar{\nu}/\bar{\mu}}, \tag{11}$$

where $x(0)$ and $y(0)$ are the initial total population size and the population gap between the two cell types, respectively. The total population size x linearly increases with increasing replication while the population gap y evolves depending on the ratio of the replication to the switch rate. In particular, the population gap is frozen at a critical condition balancing replication and switching,

$$\bar{\mu} = 2\bar{\nu}. \tag{12}$$

However, the gap increases in the replication-dominant condition ($\bar{\mu} > 2\bar{\nu}$) while it decreases in the switch-dominant condition ($\bar{\mu} < 2\bar{\nu}$).

For general cases ($\mu_1 \neq \mu_2$ and $\nu_1 \neq \nu_2$), the dynamic behaviors of x and y in Eqs. (8) and (9) can be inferred from the vector fields of $(\dot{x}, \dot{y})$ on the x-y plane (Fig. 2). Here, local slopes dy/dx on the x-y plane are defined as

$$\frac{dy}{dx} = \frac{(\Delta\mu - 2\Delta\nu) + (\bar{\mu} - 2\bar{\nu})\, y/x}{\bar{\mu} + \Delta\mu\, y/x} \tag{13}$$

by using Eqs. (8) and (9). The local slopes are invariant at a critical condition,

$$\frac{\nu_1}{\mu_1} + \frac{\nu_2}{\mu_2} = 1. \tag{14}$$

Note that this critical condition is a generalized one for the simple case $\bar{\mu} = \mu_1 = \mu_2$ and $\bar{\nu} = \nu_1 = \nu_2$ in Eq. (12).

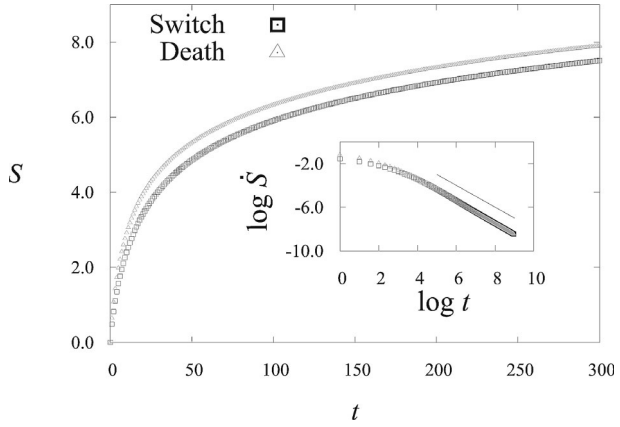

Fig. 4. Entropy production of the population dynamics. Considered are two population dynamics models: the switch (black squares) and the death (gray triangles) models. Here, the phenotypic switch of cell types in the switch model can be considered as death of one cell type and concurrent replication of another cell type in the death model. The inset plots the entropy production rate $\dot{S}$. The black solid line represents $\dot{S} = t^{-1}$. For this plot, we used $\mu_1 = 0.051$, $\mu_2 = 0.021$, $\nu_1 = 0.031$, and $\nu_2 = 0.029$ as parameter values, and $x(0) = 190$ and $y(0) = 10$ as initial conditions.

The critical condition can categorize three qualitative behaviors of the vector fields (Fig. 3(a)). In the population dynamics, we are ultimately interested in the population gap relative to the total population size, $z = y/x$. To check whether the normalized gap z converges to a certain value, we examine its time evolution

$$\begin{aligned}\dot{z} &= \frac{1}{x}(\dot{y} - \dot{x}z) \\ &= \frac{1}{x}(-\Delta\mu z^2 - 2\bar{\nu}z + \Delta\mu - 2\Delta\nu) \end{aligned} \quad (15)$$

by using Eqs. (8) and (9). Indeed, the normalized gap has a stable fixed point at

$$z^* = \frac{-\bar{\nu} + \sqrt{\bar{\nu}^2 + \Delta\mu(\Delta\mu - 2\Delta\nu)}}{\Delta\mu} \quad (16)$$

in Fig. 3(b). Note that the normalized population gap, $z = x/y = (a-b)/(a+b)$, stays in $|z| \leq 1$ and that $z^* = 0$ for the simple case $\Delta\mu = \Delta\nu = 0$. Interestingly, the normalized population gap z^* is independent of the mean replication rate $\bar{\mu} = (\mu_1 + \mu_2)/2$. As $z = x/y$ approaches z^*, the local slope dy/dx in Eq. (13) becomes $dy/dx = z^*$, regardless of $\bar{\mu}$ (Fig. 3(a)). However, the mean replication rate $\bar{\mu}$ determines the speed of convergence to the fixed point (Fig. 2).

IV. FLUCTUATIONS IN THE POPULATION DYNAMICS

The switching of cell types is hard to probe experimentally because the event may be indistinguishable from the death of one cell type and the concurrent replication of another cell type:

$$\text{A, B} \to \text{B, B} \qquad \text{(switch model)},$$

$$\text{A, B} \to \phi\text{, BB} \qquad \text{(death model)}.$$

As we derived the master equation of Eq. (1) for the switch model, we can similarly write the master equation for the death model:

$$\begin{aligned} &P(a,b;t+1) - P(a,b;t) = \\ &\mu_1 \frac{a-1}{a+b-1} P(a-1,b;t) + \mu_2 \frac{b-1}{a+b-1} P(a,b-1;t) \\ &+\nu_1 \frac{a+1}{a+b+1} P(a+1,b;t) + \nu_2 \frac{b+1}{a+b+1} P(a,b+1;t) \\ &+\nu_1 \frac{a}{a+b-1} P(a,b-1;t) + \nu_2 \frac{b}{a+b-1} P(a-1,b;t) \\ &-(\mu_1 + 2\nu_1)\frac{a}{a+b} P(a,b;t) - (\mu_2 + 2\nu_2)\frac{b}{a+b} P(a,b;t). \end{aligned} \quad (17)$$

In the switch model, the switch A→B occurs from the $(a+1, b-1)$ state to the (a,b) state in Eq. (1). In the death model, however, the death A→ ϕ occurs from the $(a+1, b)$ state to the (a,b) state, and the replication B→BB occurs from the $(a, b-1)$ state to the (a,b) state. Therefore, the switch of a cell type can be considered to be a synchronous death and replication. Note that the death rate of A cells and the concurrent replication rate of B cells are set as ν_1 in the death model, which is equivalent to the switch rate of A cells in the switch model. The same applies for ν_2.

Here, the transition rate for the concurrent replication (B→BB) is $\nu_1 a/(a+b-1)$ in Eq. (17). At first glance, it may look odd that we use a probability of selecting A cells, not B cells, among a numbers of A cells and $(b-1)$ numbers of B cells to replicate a B cell. However, this makes the death model equivalent to the switch model because when the switch A→B occurs (assuming B cells are a minor population), an additional B cell can appear. Note that the switch process makes the dominant population less dominant, and the minor population less minor. Therefore, the odd selection probability allows minor B cells to increase through replication. Finally, we derive the Fokker-Planck equation for the death model from Eq. (17), similarly to Eq. (2) after changing variables to $x = a + b$ and $y = a - b$. As expected, the drift terms v_x and v_y are exactly the same for the two models, demonstrating that the average behavior of population balance is equivalent in the switch model and the death model.

On the other hand, the diffusion terms in their Fokker-Planck equations are different (Table 1). For convenience, we define a diffusion matrix

$$D = \begin{pmatrix} D_{xx} & D_{xy} \\ D_{yx} & D_{yy} \end{pmatrix},$$

Table 1. Elements of the diffusion matrix.

	Switch model	Death model
D_{xx}	$\bar{\mu} + \Delta\mu\, z$	$\bar{\mu} + 2\bar{\nu} + (\Delta\mu + 2\Delta\nu)\, z$
D_{yy}	$\bar{\mu} + 4\bar{\nu} + (\Delta\mu + 4\Delta\nu)\, z$	$\bar{\mu} + 2\bar{\nu} + (\Delta\mu + 2\Delta\nu)\, z$
D_{xy}	$\Delta\mu + \bar{\mu}\, z$	$\Delta\mu + \bar{\mu}\, z$

where $D_{xy} = D_{yx}$. Note that the diffusion matrix is just a function of the normalized population gap $z = y/x$. The diffusion originates from fluctuations in the population dynamics. Here, the degree of fluctuations can be measured as an uncertainty in the population distribution, the *entropy*:

$$S(t) = -\int\int dxdy\, P(x, y; t) \log P(x, y; t). \qquad (18)$$

When $z \to z^*$ after a sufficiently long time, the probability distribution can be approximated by

$$P(x', y'; t) = \frac{1}{2\pi\, t\sqrt{D'_{xx} D'_{yy}}} \times \exp\Big[- \frac{(x' - v'_x\, t)^2}{2D'_{xx}\, t} - \frac{(y' - v'_y\, t)^2}{2D'_{yy}\, t} \Big], \qquad (19)$$

where primed coordinates $X' = U^{-1}X$ are chosen to diagonalize the diffusion matrix $D' = U^{-1}DU$. In the long time limit, the entropy is calculated as

$$S(t) \approx \log\Big(2\pi\, t\sqrt{D'_{xx} D'_{yy}}\Big) = \log\Big(2\pi\, t\sqrt{\det D}\Big). \qquad (20)$$

This entropy measure concludes that the death model has larger fluctuations in the population dynamics than the switch model (Fig. 4). The switch of cell type can be considered as the synchronous death of one cell type and replication of another cell type. The event synchronization can diminish fluctuations in the population dynamics, in contrast to the independent death and replication events in the death model. Nevertheless, the entropy production rate is the same in both models,

$$\dot{S} = t^{-1}. \qquad (21)$$

V. SUMMARY

We develop a population balancing model that incorporates cell replication and transdifferentiation. The stochastic model was mapped into an urn process. We found that a stationary population balance depended on the replication and the transdifferentiation rates of binary cells.

Dynamic equations for the average behavior of population balancing have been proposed to describe phenotypic changes of bacteria [14]. One distinction is that our model considers one replication/switch at a time while the previous model considers multiple replications/switches at a time. However, this distinction does not change the characteristic behavior of the population dynamics except for modifying the time scale. When multiple replications are allowed per unit time, the population dynamics is just accelerated by rescaling the time as $\Delta t' = \Delta t/x$ where x is the population size. Furthermore, if the replication and the transdifferentiation rates are very small, as is usually observed in biological tissues, the difference becomes negligible.

Finally, our analysis based on the Fokker-Planck equation proposed a method to distinguish the switch of cell types from the death of one cell type and the concurrent replication of another cell type. Although the two scenarios can equivalently describe the average behavior of the population dynamics, the switch model generates fewer fluctuations in the population dynamics than the death model because the event of switching can be considered as synchronous death and replication events. In practice, experimental data would be the total population size and the population gap between two cell types, $x(t) \pm \delta x(t)$ and $y(t) \pm \delta y(t)$, respectively. Through fitting the data to the model of Eqs. (8) and (9), we can estimate the likelihood values of the model parameters, $(\mu_1, \mu_2, \nu_1, \nu_2)$, which are common in the switch and the death models. Once the parameter values are determined, calculating the entropy of each model, Eq. (20), is straightforward. Then, the predicted entropies can be directly compared with the measured entropies based on the covariance matrix from data uncertainties, $(\delta x(t),\ \delta y(t))$. Although the switch and the death models are the simplest for describing the population dynamics with two species, we cannot completely rule out alternative models including additional processes.

ACKNOWLEDGMENTS

This research was supported by the Basic Science Research Program through the National Foundation of Korea funded by the Ministry of Science, ICT & Future Planning (No. 2013R1A1A1006655) and by the Max Planck Society, the Korea Ministry of Education, Science and Technology, Gyeongsangbuk-Do and Pohang City.

REFERENCES

[1] G. Eguchi and R. Kodama, Curr. Opin. Cell Biol. **5**, 1023 (1993)
[2] C.-N. Shen, Z. D. Burke and D. Tosh, Organogenesis **1**, 36 (2004).
[3] J. Ladewig, P. Koch and O. Brüstle, Nat. Rev. Mol. Cell Biol. **14**, 225 (2013).
[4] S. Thowfeequ, E.-J. Myatt and D. Tosh, Dev. Dynam. **236**, 3208 (2007).

[5] S. Sisakhtnezhad and M. M. Matin, Cell Tissue Res. **348**, 379 (2012).
[6] J. M. Slack, Nat. Rev. Mol. Cell Biol. **8**, 369 (2007)
[7] F. Thorel, V. Népote, I. Avril, K. Kohno, R. Desgraz, S. Chera and P. L. Herrera, Nature **464**, 1149 (2010).
[8] Q. Zhou, J. Brown, A. Kanarek, J. Rajagopal and D. A. Melton, Nature **455**, 627 (2004).
[9] M. Ieda, J.-D. Fu, P. Delgado-Olguin, V. Vedantham, Y. Hayashi, B. G. Bruneau and D. Srivastava, Cell **142**, 375 (2010).
[10] L. Qiang *et al.*, Cell **146**, 359 (2011)
[11] K. S. Zaret, Nat. Rev. Genet. **9**, 329 (2008).
[12] J. Hanna, K. Saha, B. Pando, J. van Zon, C. J. Lengner, M. P. Creyghton, A. van Oudenaarden and R. Jaenisch, Nature **462**, 595 (2009).
[13] H.-X. Zhou, Q. Rev. Biophys. **43**, 219 (2010).
[14] M. Thattai and A. van Oudenaarden, Genetics **167**, 523 (2004).
[15] N. L. Johnson and S. Kotz, *Urn models and their application: an approach to modern discrete probability theory* (Wiley, New York, 1977), pp. 176-209.
[16] D. R. Cox and H. D. Miller, *The theory of stochastic processes* (Chapman and Hall/CRC, Boca Raton, 1977).